Chaos, Solitons and Fractals 167 (2023) 113048

Contents lists available at ScienceDirect

Chaos, Solitons and Fractals

journal homepage: www.elsevier.com/locate/chaos

Mathematical modelling of clonorchiasis with human treatment and fish vaccination versus snail control

Mainul Haque [a,*], Fahad Al Basir [b], Ezio Venturino [c], Abdulhalim Saeed [d], Stacey R. Smith? [e]

[a] School of Mathematical Sciences, University of Nottingham Ningbo China, PR China
[b] Department of Mathematics, Asansol Girls' College, India
[c] Dipartimento di Matematica, Università di Torino, Italy
[d] Faculty of Science and Engineering, University of Nottingham Ningbo China, PR China
[e] Department of Mathematics and Faculty of Medicine, The University of Ottawa, Canada

ARTICLE INFO

Keywords:
Clonorchiasis
Fish vaccination
Impulsive differential equation
Stability analysis
Basic reproduction number

ABSTRACT

Clonorchiasis is an important food-borne parasitic disease that has been largely understudied. We examine the dynamics of clonorchiasis with human treatment and fish vaccination versus snail control. Four mathematical models are proposed and analysed, both analytically and numerically. We show that fish vaccination is a valid method of control and derive the maximal period of molluscicide application in order to control the snail populations. It follows that a variety of methods may be necessary to control clonorchiasis.

1. Introduction

The liver fluke *Clonorchis sinensis* is a high-risk pathogenic parasitic helminth that is predominantly endemic in Asian countries — including Korea, China, Taiwan, Vietnam and the far eastern parts of Russia — and is still actively transmitted, causing the disease condition clonorchiasis, which is associated with urinary bladder cancer [1]. Currently, more than 35 million people are infected with clonorchiasis [2], with 750 million at risk [3]. The public-health importance of liver-fluke infections, especially clonorchiasis, has been neglected for decades, despite a persistent and growing number of infections and corresponding disease burden [4].

Snails act as a first intermediate host, while freshwater fish act as a secondary intermediate host [4]. Freshwater snails ingest eggs laid by hermaphrodite adult worms and produce cercariae, which escape from the snails and adhere to freshwater fish [5]. When people eat raw or undercooked fish, metacercarie separate from the flesh through gastric digestion, and juvenile flukes migrate to the bile ducts, where they become adult flukes [6]. Eggs laid by hermaphrodite adult worms reach the human intestine and are eliminated with the faeces [7]. The egg-laying capacity of an adult *C. sinensis* fluke has been estimated at around 4000 eggs per worm per day [8].

Piscivorous animals, especially cats and dogs (both wild or reared as pets or guardians), can also serve as reservoir hosts for *C. sinensis*; these animals are widely distributed and can maintain the lifecycle of the parasite in endemic areas without involvement of people [4]. Infection in cats is higher than dogs, possibly due to their preference for eating fish [9].

Praziquantel is virtually the only drug for treating *C. sinensis* infections and has been recommended by the World Health Organization (WHO) for more than 30 years [10]. Monotherapy is 70%–90% effective, but this is a potentially dangerous situation if drug resistance should emerge [11]; possible emergence of praziquantel-resistant strains (or isolates) of *S. mansoni* and *S. japonicum* has been documented in the laboratory [12], raising the spectre that resistance may emerge against *C. sinensis*. Another drug, Albendazole, requires long treatment courses over multiple days [13] and has a high rate of egg reduction but low cure rates [14] and so is rarely used [11]. Reinfection in animals is common, making practical treatment of cats and dogs infeasible [15].

No commercially produced or effective vaccine is available for the treatment of *C. sinensis* infection in human or other hosts as of yet. However, the possibility of developing a fish vaccine, in combination with the use of non-polluted water for the culture of fish, has been proposed [16]. Snail control has also been suggested as a way to interrupt the transmission cycle [17], specifically with predator fish [4], as widespread molluscicide is not recommended [18]. Other environmental controls include removing toilets over fish ponds — although complete removal of faecal contamination is not feasible [4] — or culturally sensitive education aimed at raising awareness of the transmission cycle and stimulating behaviour changes that discourage consumption of raw fish and improve sanitary practices [18]. The

* Corresponding author.
E-mail address: Mainul.Haque@nottingham.edu.cn (M. Haque).

https://doi.org/10.1016/j.chaos.2022.113048
Received 30 September 2022; Received in revised form 2 December 2022; Accepted 19 December 2022
Available online 3 January 2023

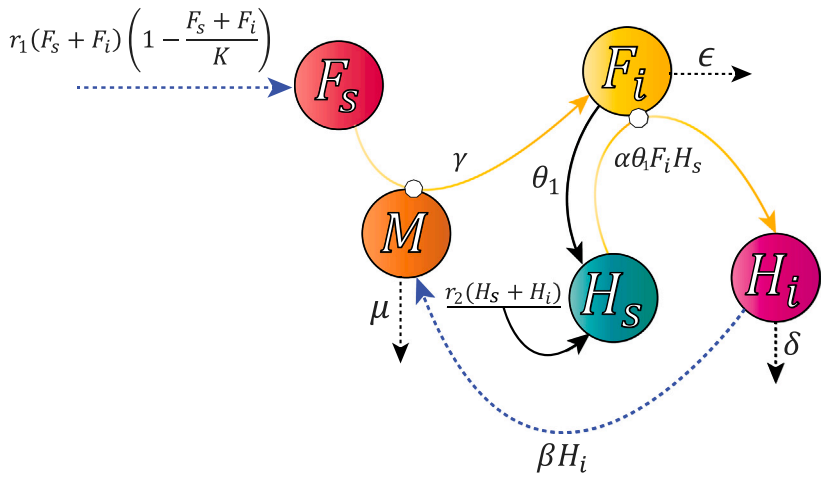

Fig. 1. Schematic diagram of model (2.1) of clonorchiasis with human treatment and fish vaccination versus snail control.

cost-effectiveness of intervention measures in China has been examined for chemotherapy, education and environmental control, with chemotherapy proving to be the most cost-effective strategy [19].

Only a handful of models have been developed for clonorchiasis. Song and Kang [20] used a mathematical analysis of age prevalence to determine egg-positive rates of clonorchiasis and developed catalytic curves for two study regions in Korea. Keiser and Utzinger [21] used a random-effects model to determine relative risk calculations for several studies of foodborne trematodiases, including *C. sinensis*, in order to determine the effect of the proximity to freshwater bodies. They showed that residents living near fresh water have a 2.15-fold higher risk for infections compared to people living further from the water. Qian et al. [22] used Monte Carlo simulations to determine overall disability weights for *C. sinensis* infection. They showed that the disability weights differed by sex and age and determined a correlation between disability and infection intensity. Lai [23] developed Bayesian geostatistical logistic regression models with location-specific random effects to obtain spatially explicit *C. sinensis* risk estimates for China in order to identify areas of high priority for control. Yuan et al. [17] developed an SEIR model for humans, with susceptible and infected snails and fish, along with *C. sinensis* eggs and cercariae, with predation of fish. They found the reproduction number and used data from China and a sensitivity analysis to show that drug treatment of humans alone would not be enough to control *C. sinensis*. Gao et al. [24] developed a model that assessed intervention techniques of snail control, health education and chemotherapy in China. They found that strengthening health education and improving faeces management would make moderate gains, but the most important tool was snail control. Zhang et al. [25] presented a model of clonorchiasis that included three time delays and found that breaking the life cycle of *Clonorchis sinensis* would be more effective than treating the disease.

Here, we introduce several mathematical models, which we develop in order to consider possible biological scenarios. Our main purpose is to investigate biological factors that influence and control invasion, persistence and variability of the disease in natural ecosystems by comparing their dynamics.

2. Model I: The baseline model

First, we consider fish F_i, humans H_i and infected molluscs M, with the worms, eggs and parasites not explicitly incorporated in the model. We assume that susceptible fish F_s grow logistically, since the infection is not passed vertically. Transmission between species is described by a mass-action process, as we can assume there is no selectivity and that populations are well-mixed.

Humans will consume both susceptible and infected fish, F_i, reducing each of their populations, while we add in a linear death rate to the infected classes. Susceptible humans can become infected upon eating infected fish, while the recruitment rate of infected molluscs is proportional to the number of infected humans. A schematic diagram is provided by Fig. 1. Note that δ represents both the natural and the disease-related mortality in humans.

$$\frac{dF_s}{dt} = r_1(F_s+F_i)\left(1-\frac{F_s+F_i}{k_1}\right) - \theta_1 F_s(H_s+H_i) - \gamma F_s M, \tag{2.1a}$$

$$\frac{dF_i}{dt} = \gamma F_s M - \theta_1 F_i(H_s+H_i) - \epsilon F_i, \tag{2.1b}$$

$$\frac{dH_s}{dt} = r_2(H_s+H_i) - \alpha\theta_1 F_i H_s, \tag{2.1c}$$

$$\frac{dH_i}{dt} = \alpha\theta_1 F_i H_s - \delta H_i, \tag{2.1d}$$

$$\frac{dM}{dt} = \beta H_i - \mu M. \tag{2.1e}$$

First, we examine the local stability of system (2.1). We write $J_k^I = J$ evaluated at E_k^I, $k = 0, 1, 2$. System (2.1) has three steady states: E_0, E_1 and E_2, where

$$E_0^I : (M, F_i, F_s, H_i, H_s) = (0, 0, 0, 0, 0),$$
$$E_1^I : (M, F_i, F_s, H_i, H_s) = \left(0, 0, k_1, 0, 0\right),$$
$$E_2^I : (M, F_i, F_s, H_i, H_s) = \left(\frac{\beta r_2 R_1}{(\delta - r_2)\mu}, \frac{\delta r_2}{\alpha\theta_1(\delta - r_2)}, \frac{\delta\mu(\delta R_1\theta_1 + \delta\epsilon - \epsilon r_2)}{\alpha\beta\gamma R_1\theta_1(\delta - r_2)}, \frac{r_2 R_1}{\delta - r_2}, R_1\right),$$

where R_1 is a positive root of the equation $\sum_0^3 Y_i Z^i = 0$, with Y_i given by

$$Y_3 = \alpha\beta^2\delta\gamma^2 k_1 r_2 {\theta_1}^2 + \alpha\beta\delta^2\gamma\mu k_1 {\theta_1}^3, \tag{2.2a}$$

$$\begin{aligned} Y_2 = (&\alpha\beta^2\delta\epsilon\gamma^2 k_1 r_2\theta_1 - \alpha\beta^2\delta\gamma^2 k_1 r_1 r_2\theta_1 - \alpha\beta^2\epsilon\gamma^2 k_1 {r_2}^2\theta_1 \\ &+ \alpha\beta^2\gamma^2 k_1 r_1 {r_2}^2\theta_1 + \alpha\beta\delta^2\epsilon\gamma\mu k_1{\theta_1}^2 + \alpha\beta\delta^2\gamma\mu\psi k_1{\theta_1}^2 \\ &- \alpha\beta\delta^2\gamma\mu k_1 r_1{\theta_1}^2 - \alpha\beta\delta\epsilon\gamma\mu k_1 r_2{\theta_1}^2, \\ &- \alpha\beta\delta\gamma\mu\psi k_1 r_2{\theta_1}^2 + \alpha\beta\delta\gamma\mu k_1 r_1 r_2{\theta_1}^2 + \beta^2\delta\gamma^2 r_1 {r_2}^2 \\ &+ 2\beta\delta^2\gamma\mu r_1 r_2\theta_1 + \delta^3\mu^2 r_1{\theta_1}^2), \end{aligned} \tag{2.2b}$$

$$\begin{aligned} Y_1 = (&\alpha\beta\delta^2\epsilon\gamma\mu\psi k_1\theta_1 - \alpha\beta\delta^2\epsilon\gamma\mu k_1 r_1\theta_1 - 2\alpha\beta\delta\epsilon\gamma\mu\psi k_1 r_2\theta_1, \\ &+ 2\alpha\beta\delta\epsilon\gamma\mu k_1 r_1 r_2\theta_1 + \alpha\beta\epsilon\gamma\mu\psi k_1 {r_2}^2\theta_1 - \alpha\beta\epsilon\gamma\mu k_1 r_1 {r_2}^2\theta_1, \\ &+ 2\beta\delta^2\epsilon\gamma\mu r_1 r_2 - 2\beta\delta\epsilon\gamma\mu r_1 {r_2}^2 + 2\delta^3\epsilon\mu^2 r_1\theta_1 - 2\delta^2\epsilon\mu^2 r_1 r_2\theta_1), \end{aligned} \tag{2.2c}$$

$$Y_0 = \delta^3\epsilon^2\mu^2 r_1 - 2\delta^2\epsilon^2\mu^2 r_1 r_2 + \delta\epsilon^2\mu^2 r_1 {r_2}^2. \tag{2.2d}$$

The equation $\sum_0^3 Y_i Z^i = 0$ has exactly one real positive root if $G^2+4H^3>0$, it has two equal roots if $G^2+4H^3=0$, and it has three distinct real roots if $G^2+4H^3>0$, where $G = {Y_1}^2 Y_4 - 3Y_1Y_2Y_3 + 2{Y_2}^3$, $H = Y_1Y_3 - {Y_2}^2$. Using Cardan's method, we obtain that the root is $\frac{1}{Y_1}(q - \frac{H}{q} - Y_2)$, where q denotes one of the three values of $[\frac{1}{2}(-G + \sqrt{G^2+4H^3})^{\frac{1}{3}}]$. The condition $G^2+4H^3=0$ yields two equal roots, and $G^2+4H^3=0$ gives three distinct real roots; by Cardan's method, we can obtain the roots. In a subsequent section, we will obtain these roots using numerical simulations.

The general Jacobian matrix of system (2.1) is

$$J^I = \begin{bmatrix} j_{11} & j_{12} & -\theta_1 F_s & -\theta_1 F_s & -\gamma F_s \\ \gamma M & -\theta_1 (H_s + H_i) - \epsilon & -\theta_1 F_i & -\theta_1 F_i & \gamma F_s \\ 0 & -\alpha \theta_1 H_s & j_{331} & j_{34} & 0 \\ 0 & \alpha \theta_1 H_s & \alpha \theta_1 F_i & -\delta & 0 \\ 0 & 0 & 0 & \beta & -\mu \end{bmatrix},$$

where j_{11}, j_{12}, j_{33} and j_{34} are defined as follows:

$$j_{11} = r_1\left(1 - \frac{F_s+F_i}{k_1}\right) - \frac{r_1(F_s+F_i)}{k_1} - \theta_1(H_s+H_i) - \gamma M,$$
$$j_{12} = r_1\left(1 - \frac{F_s+F_i}{k_1}\right) - \frac{r_1(F_s+F_i)}{k_1},$$
$$j_{33} = r_2\left(1 - \frac{H_s+H_i}{k_2}\right) - \frac{r_2(H_s+H_i)}{k_2} - \alpha\theta_1 F_i,$$
$$j_{34} = r_2\left(1 - \frac{H_s+H_i}{k_2}\right) - \frac{r_2(H_s+H_i)}{k_2}.$$

The general Jacobian matrix of system (2.1) is

$$J^I = \begin{bmatrix} j_{11} & j_{12} & -\theta_1 F_s & -\theta_1 F_s & -\gamma F_s \\ \gamma M & -\theta_1 (H_s + H_i) - \epsilon & -\theta_1 F_i & -\theta_1 F_i & \gamma F_s \\ 0 & -\alpha \theta_1 H_s & j_{331} & j_{34} & 0 \\ 0 & \alpha \theta_1 H_s & \alpha \theta_1 F_i & -\delta & 0 \\ 0 & 0 & 0 & \beta & -\mu \end{bmatrix},$$

where j_{11}, j_{12}, j_{33} and j_{34} are defined as follows:

$$j_{11} = r_1\left(1 - \frac{F_s+F_i}{k_1}\right) - \frac{r_1(F_s+F_i)}{k_1} - \theta_1(H_s+H_i) - \gamma M,$$
$$j_{12} = r_1\left(1 - \frac{F_s+F_i}{k_1}\right) - \frac{r_1(F_s+F_i)}{k_1},$$
$$j_{33} = r_2\left(1 - \frac{H_s+H_i}{k_2}\right) - \frac{r_2(H_s+H_i)}{k_2} - \alpha\theta_1 F_i,$$
$$j_{34} = r_2\left(1 - \frac{H_s+H_i}{k_2}\right) - \frac{r_2(H_s+H_i)}{k_2}.$$

The Jacobian matrix at E_0^I is given by

$$J_0^I = \begin{bmatrix} -\psi + r_1 & r_1 & 0 & 0 & 0 \\ 0 & -\epsilon & 0 & 0 & 0 \\ 0 & 0 & r_2 & r_2 & 0 \\ 0 & 0 & 0 & -\delta & 0 \\ 0 & 0 & 0 & \beta & -\mu \end{bmatrix}.$$

The eigenvalues of J_0^I are $-\psi + r_1$, $-\epsilon$, r_2, $-\delta$, $-\mu$. Since $r_2 > 0$, E_0 is always unstable. The Jacobian matrix at E_1^I is given by

$$J_1^I = \begin{bmatrix} \psi - r_1 & 2\psi - r_1 & \frac{\theta_1 k_1(\psi - r_1)}{r_1} & \frac{\theta_1 k_1(\psi - r_1)}{r_1} & \frac{\gamma k_1(\psi - r_1)}{r_1} \\ 0 & -\epsilon & 0 & 0 & -\frac{\gamma k_1(\psi - r_1)}{r_1} \\ 0 & 0 & r_2 & r_2 & 0 \\ 0 & 0 & 0 & -\delta & 0 \\ 0 & 0 & 0 & \beta & -\mu \end{bmatrix}.$$

The eigenvalues of J_1^I are $\psi - r_1$, $-\epsilon$, r_2, $-\delta$, $-\mu$. E_1^I is unstable, since $r_2 > 0$. Note that the stability of E_2^I can only be shown numerically.

Since E_0 is always unstable, extinction of all species is impossible. The details of the stability analysis shows that the extinction of all species is impossible due to the positive human net birth rate r_2. Finally, the stability of E_2 is conditional.

To illustrate our results, we ran several numerical simulations. Some parameter values in Table 1 are taken from the ecology literature, and some data are estimated. Fig. 2 shows the numerical solution of system (2.1). Solutions oscillate before reaching a coexistence equilibrium.

3. Model II: Fish vaccination and linear human growth

Here, we modify model (2.1) by considering vaccination of fish. See Fig. 3. Let ψ be the rate of vaccination of susceptible fish and F_v be the vaccinated fish population.

With these assumptions, model (2.1) reduces to

$$\frac{dF_s}{dt} = r_1(F_s+F_i+F_v)\left(1 - \frac{F_s+F_i+F_v}{k_1}\right) - \theta_1 F_s(H_s+H_i) - \gamma F_s M - \psi F_s, \tag{3.1a}$$
$$\frac{dF_i}{dt} = \gamma F_s M - \theta_1 F_i(H_s+H_i) - \epsilon F_i, \tag{3.1b}$$
$$\frac{dF_v}{dt} = \psi F_s - \theta_1 F_v(H_s+H_i) - \phi F_v, \tag{3.1c}$$
$$\frac{dH_s}{dt} = r_2(H_s+H_i) - \alpha\theta_1 F_i H_s + \omega H_i, \tag{3.1d}$$
$$\frac{dH_i}{dt} = \alpha\theta_1 F_i H_s - \delta H_i - \omega H_i, \tag{3.1e}$$
$$\frac{dM}{dt} = \beta H_i - \mu M. \tag{3.1f}$$

System (4.1) possesses the following equilibrium points:

$$E_0^{II} : (M, F_i, F_s, F_v, H_i, H_s) = \left(0,0,0,0,0,0\right),$$
$$E_1^{II} : (M, F_i, F_s, F_v, H_i, H_s) = \left(0, 0, \frac{(-\psi\phi + \phi r_1 + \psi r_1)k_1\phi}{(\phi^2 + 2\psi\phi + \psi^2)r_1}, \frac{(-\psi\phi + \phi r_1 + \psi r_1)\psi k_1}{(\phi^2 + 2\psi\phi + \psi^2)r_1}, 0, 0\right),$$
$$E_2^{II} : (M, F_i, F_s, F_v, H_i, H_s) = \left(\frac{\beta r_2 R_2}{(\delta - r_2)\mu}, \frac{r_2(\delta+\omega)}{\alpha\theta_1(\delta - r_2)}, \frac{(R_2\delta^2\theta_1 + R_2\delta\omega\theta_1 + \delta^2\epsilon + \delta\epsilon\omega - \delta\epsilon r_2 - \epsilon\omega r_2)\mu}{(\delta - r_2)\theta_1 R_2\gamma\alpha\beta}, \frac{\mu\psi(R_2\delta^2\theta_1 + R_2\delta\omega\theta_1 + \delta^2\epsilon + \delta\epsilon\omega - \delta\epsilon r_2 - \epsilon\omega r_2)}{(R_2\delta\theta_1 + \delta\phi - r_2\phi)\gamma\alpha\beta R_2\theta_1}, \frac{r_2 R_2}{\delta - r_2}, R_2\right),$$

where R_2 is a positive root of the equation $\sum_0^5 Y_i Z^i = 0$, with Y_i as in Eqs. (2.2).

The equilibrium point E_0^{II} always exists. However, the equilibrium point E_1^{II} exists if and only if $r_1 > r_1^{II}$, where $r_1^{II} = \frac{\psi\phi}{\psi+\phi}$; that is, the birth rate of the fish population is greater than the threshold r_1^{II}. Note that the threshold increases with ψ, so fish vaccination is a valid method of control.

Table 1
Parameter values used in numerical simulations.

Parameter	Description	Value (unit)	Reference
r_1	Intrinsic growth rate of fish	0.2 day^{-1}	[4,26]
r_2	Intrinsic growth rate of humans	0.01 day^{-1}	[4,27]
k_1	Carrying capacity of fish	1000 m^{-2}	[17,26]
k_2	Carrying capacity of humans	500 km^{-2}	[17,26]
γ	Infection rate of fish	0.0025 day^{-1}	[28,29]
θ_1	Consumption rate of fish by humans	0.025 $humans^{-1}$ day^{-1}	[29,30]
ψ	Rate of vaccination	0.1 day^{-1}	[31,32]
α	Infection rate of humans due to consumption	0.005 day^{-1}	[17,29]
β	Growth rate of infective molluscs	0.5 day^{-1}	[4,27]
μ	Mortality rate of molluscs	1 day^{-1}	[33,34]

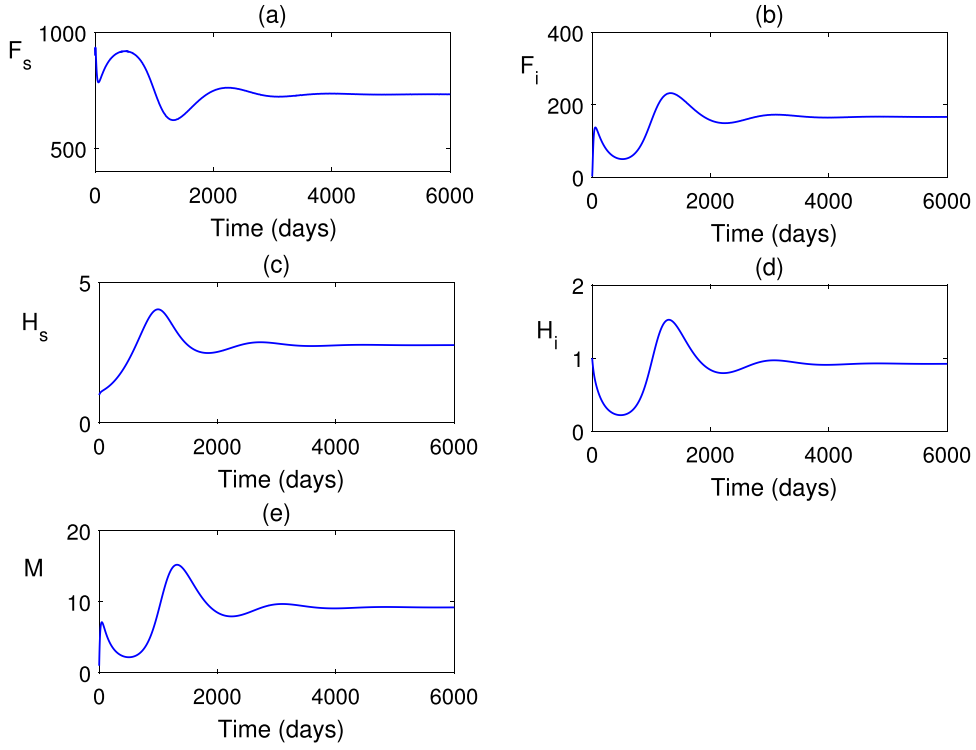

Fig. 2. Numerical solution of system (2.1) using the parameters given in Table 1. Note the different scales on the y-axes.

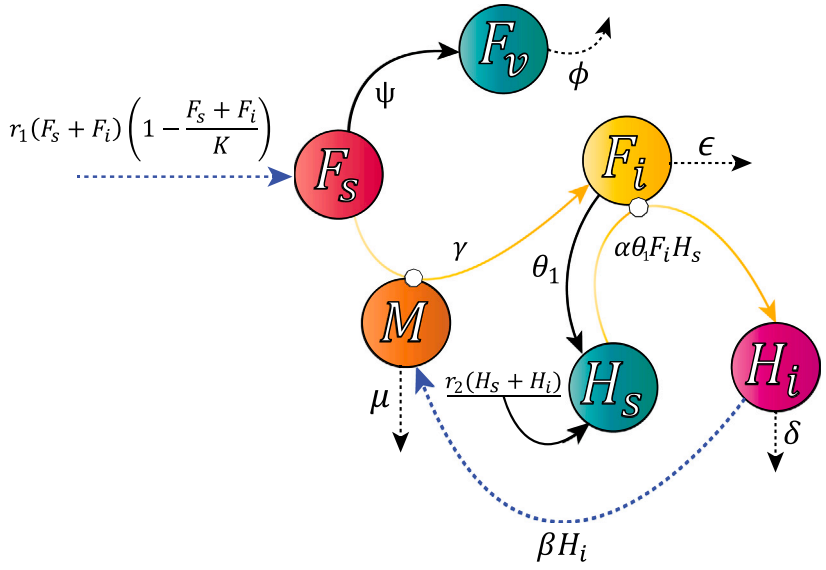

Fig. 3. Schematic diagram of model (3.1) of clonorchiasis with human treatment and fish vaccination versus snail control.

The Jacobian matrix at E_0 is given by

$$J^{II} = \begin{bmatrix} -\frac{\psi k_1 + 2F_v r_1 - k_1 r_1}{k_1} & -\frac{r_1(2F_v - k_1)}{k_1} & -\frac{r_1(2F_v - k_1)}{k_1} & 0 & 0 & 0 \\ 0 & -\epsilon & 0 & 0 & 0 & 0 \\ \psi & 0 & -\phi & -\theta_1 F_v & -\theta_1 F_v & 0 \\ 0 & 0 & 0 & r_2 & r_2 + \omega & 0 \\ 0 & 0 & 0 & 0 & -\delta - \omega & 0 \\ 0 & 0 & 0 & 0 & \beta & -\mu \end{bmatrix}.$$

The eigenvalues of J_0^{II} are

$$-\epsilon, r_2, -\delta - \omega, -\mu, \pm\frac{\phi k_1 + \psi k_1 + 2r_1 F_v - r_1 k_1 + \sqrt{\Gamma_2}}{2k_1},$$

where

$$\Gamma_2 = \phi^2 {k_1}^2 - 2\phi\psi {k_1}^2 - 4\phi F_v k_1 r_1 + 2\phi k_1^2 r_1 + \psi^2 {k_1}^2 - 4\psi F_v k_1 r_1 + 2\psi k_1^2 r_1 + 4{F_v}^2 {r_1}^2 - 4F_v k_1 {r_1}^2 + k_1^2 {r_1}^2.$$

The Jacobian matrix at E_1^{II} is given by

$$J_1^{II} = \begin{bmatrix} a_{11} & a_{12} & a_{13} & a_{14} & a_{15} & a_{16} \\ 0 & -\epsilon & 0 & 0 & 0 & a_{26} \\ \psi & 0 & -\phi & a_{34} & a_{35} & 0 \\ 0 & 0 & 0 & r_2 & r_2 + \omega & 0 \\ 0 & 0 & 0 & 0 & -\delta - \omega & 0 \\ 0 & 0 & 0, & 0 & \beta & -\mu \end{bmatrix},$$

where

$$a_{11} = \frac{\phi\psi - \phi r_1 - \psi^2 - \psi r_1}{\phi + \psi}, \qquad a_{12} = \frac{2\phi\psi - \phi r_1 - \psi r_1}{\phi + \psi},$$
$$a_{13} = \frac{2\phi\psi - \phi r_1 - \psi r_1}{\phi + \psi}, \qquad a_{14} = \frac{\theta_1\left(\phi\psi - \phi r_1 - \psi r_1\right)k_1\phi}{\left(\phi^2 + 2\phi\psi + \psi^2\right)r_1},$$
$$a_{15} = \frac{\theta_1\left(\phi\psi - \phi r_1 - \psi r_1\right)k_1\phi}{\left(\phi^2 + 2\phi\psi + \psi^2\right)r_1}, \qquad a_{16} = \frac{\gamma\left(\phi\psi - \phi r_1 - \psi r_1\right)k_1\phi}{\left(\phi^2 + 2\phi\psi + \psi^2\right)r_1},$$
$$a_{26} = -\frac{\gamma\left(\phi\psi - \phi r_1 - \psi r_1\right)k_1\phi}{\left(\phi^2 + 2\phi\psi + \psi^2\right)r_1}, \qquad a_{34} = \frac{\theta_1\left(\phi\psi - \phi r_1 - \psi r_1\right)\psi k_1}{\left(\phi^2 + 2\phi\psi + \psi^2\right)r_1},$$
$$a_{35} = \frac{\theta_1\left(\phi\psi - \phi r_1 - \psi r_1\right)\psi k_1}{\left(\phi^2 + 2\phi\psi + \psi^2\right)r_1}.$$

The eigenvalues of J_1^{II} are

$$-\omega, -\epsilon, r_2, -\delta, -\mu, \frac{-\phi^2 - \phi r_1 - \psi^2 - \psi r_1 + \sqrt{\Gamma_1}}{2\phi + 2\psi},$$

where

$$\Gamma_1 = \phi^4 + 4\phi^3\psi - 2\phi^3 r_1 + 10\phi^2\psi^2 - 10\phi^2\psi r_1 + \phi^2 {r_1}^2 + 4\phi\psi^3 - 10\phi\psi^2 r_1 + 2\phi\psi {r_1}^2 + \psi^4 - 2\psi^3 r_1 + \psi^2 {r_1}^2.$$

Therefore E_0^{II} and E_1^{II} is always unstable. This instability is due to the human birth rate $r_2 > 0$. The stability of E_2^{II} can only be shown numerically. This means that human births save the molluscs and infected fish from extinction, along with the human species itself.

Fig. 4 illustrates the time-dependent solution of system (3.1). In this case, there are damped oscillations, and the system approaches a coexistence steady state.

4. Model III: Logistic human growth without intervention

As a refinement of our baseline model, we assume that the susceptible humans grow logistically. Since the infection is not passed vertically, model (2.1) in this case becomes

$$\frac{dF_s}{dt} = r_1(F_s + F_i)\left(1 - \frac{F_s + F_i}{k_1}\right) - \theta_1 F_s(H_s + H_i) - \gamma F_s M, \tag{4.1a}$$
$$\frac{dF_i}{dt} = \gamma F_s M - \theta_1 F_i(H_s + H_i) - \epsilon F_i, \tag{4.1b}$$
$$\frac{dH_s}{dt} = r_2(H_s + H_i)\left(1 - \frac{H_s + H_i}{k_2}\right) - \alpha\theta_1 F_i H_s, \tag{4.1c}$$
$$\frac{dH_i}{dt} = \alpha\theta_1 F_i H_s - \delta H_i, \tag{4.1d}$$
$$\frac{dM}{dt} = \beta H_i - \mu M. \tag{4.1e}$$

System (4.1) has four biologically feasible steady states when the molluscs are eradicated:

$$E_0^{III} : (M, F_i, F_s, H_i, H_s) = (0, 0, 0, 0, 0),$$
$$E_1^{III} : (M, F_i, F_s, H_i, H_s) = (0, 0, k_1, 0, 0),$$
$$E_2^{III} : (M, F_i, F_s, H_i, H_s) = (0, 0, 0, 0, k_2),$$
$$E_3^{III} : (M, F_i, F_s, H_i, H_s) = (0, 0, \frac{k_1(r_1 - k_2\theta_1)}{r_1}, 0, k_2).$$

Since E_0^{III} and E_1^{III} are always unstable, extinction of all species is not possible for positive initial conditions. It is possible that susceptible humans thrive while the remaining species become extinct if $\theta_1 > \frac{r_1}{k_2}$ (or $R_0^{III} < 1$ where $R_0^{III} = \frac{r_1}{\theta_1 k_2}$). Indeed, the latter is the condition for which E_2^{III} is stable. If the fish consumption or the predation rate by the human population is greater than a threshold, then all species go extinct except for susceptible humans, and the epidemic is avoided.

Theorem 4.1. *The disease-free equilibrium E_3^{III} is stable if and only if $r_1 - k_2\theta_1 > 0$ and*

$$R_0 = \frac{\gamma k_1 k_2 \theta\beta(r_1 - k_2\theta_1)}{r_1(k_2\theta_1 + \epsilon)r_2\mu} < 1.$$

Proof. The Jacobian matrix at E_3^{III} is given by

$$J_3^{III} = \begin{bmatrix} k_2\theta_1 - r_1 & 2k_2\theta_1 - r_1 & \frac{k_1\theta_1(k_2\theta_1 - r_1)}{r_1} & \frac{k_1\theta_1(k_2\theta_1 - r_1)}{r_1} & \frac{\gamma k_1(k_2\theta_1 - r_1)}{r_1} \\ 0 & -k_2\theta_1 - \epsilon & 0 & 0 & -\frac{\gamma k_1(k_2\theta_1 - r_1)}{r_1} \\ 0 & -\alpha k_2\theta_1 & -r_2 & -r_2 & 0 \\ 0 & \alpha k_2\theta_1 & 0 & -\delta & 0 \\ 0 & 0 & 0 & \beta & -\mu \end{bmatrix}.$$

The two eigenvalues of J_3^{III} are $k_2\theta_1 - r_1 < 0$, $-r_2 < 0$. The remaining eigenvalues satisfy the following cubic:

$$\rho^3 + (\delta + \mu + k_2\theta_1 + \epsilon)\rho^2 + \{(r_2 + \mu)(k_2\theta_1 + \epsilon) + r_2\mu\}\rho + r_1(k_2\theta_1 + \epsilon)r_2\mu - \gamma k_1 k_2\theta\beta(r_1 - k_2\theta_1) = 0. \tag{4.3}$$

Since the coefficients of Eq. (4.3) satisfy $(\delta + \mu + k_2\theta_1 + \epsilon) > 0$, $(r_2 + \mu)(k_2\theta_1 + \epsilon) + r_2\mu > 0$, using Routh–Hurwitz criterion, all roots of Eq. (4.3) will be negative or have negative real parts if and only if the last coefficient is positive; i.e.,

$$r_1(k_2\theta_1 + \epsilon)r_2\mu - \gamma k_1 k_2\theta\beta(r_1 - k_2\theta_1) > 0.$$

Fig. 5 describes the numerical simulation of system (4.1). In this case, there are essentially no oscillations, and the system approaches a coexistence equilibrium.

5. Model IV: Molluscicide and logistic human growth

We now build on the previous models to add molluscicide to control the snail population, while including logistic growth for humans. The model becomes

$$\frac{dF_s}{dt} = r_1(F_s + F_i + F_v)\left(1 - \frac{F_s + F_i + F_v}{k_1}\right) - \theta_1 F_s(H_s + H_i) - \gamma F_s M - \psi F_s, \tag{5.1a}$$
$$\frac{dF_i}{dt} = \gamma F_s M - \theta_1 F_i(H_s + H_i) - \epsilon F_i, \tag{5.1b}$$

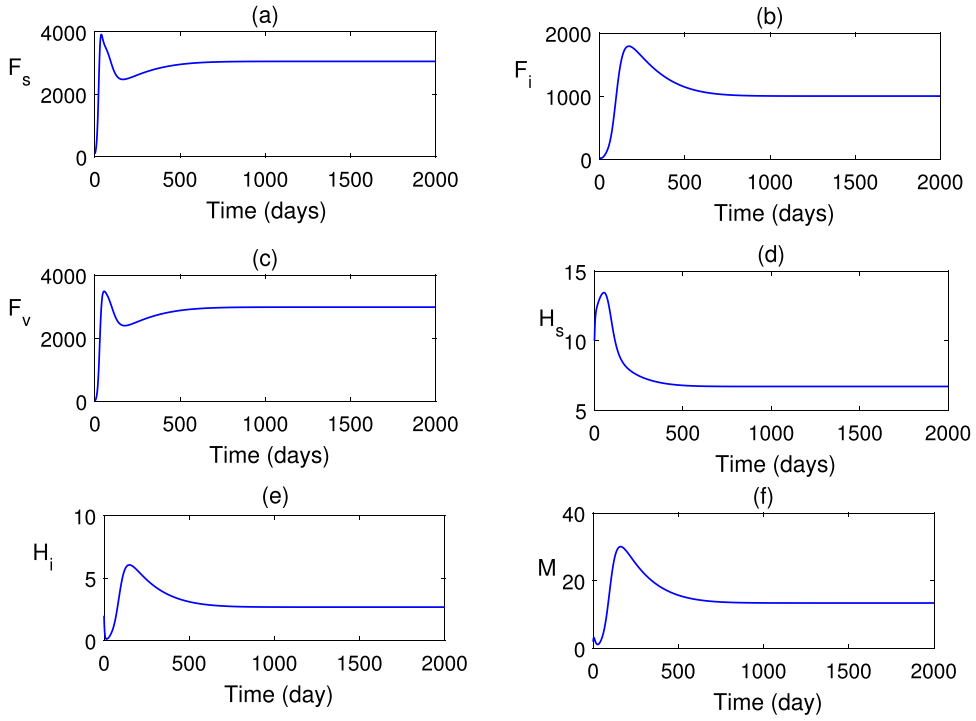

Fig. 4. Numerical solution of the system (3.1) using the parameters given in Table 1.

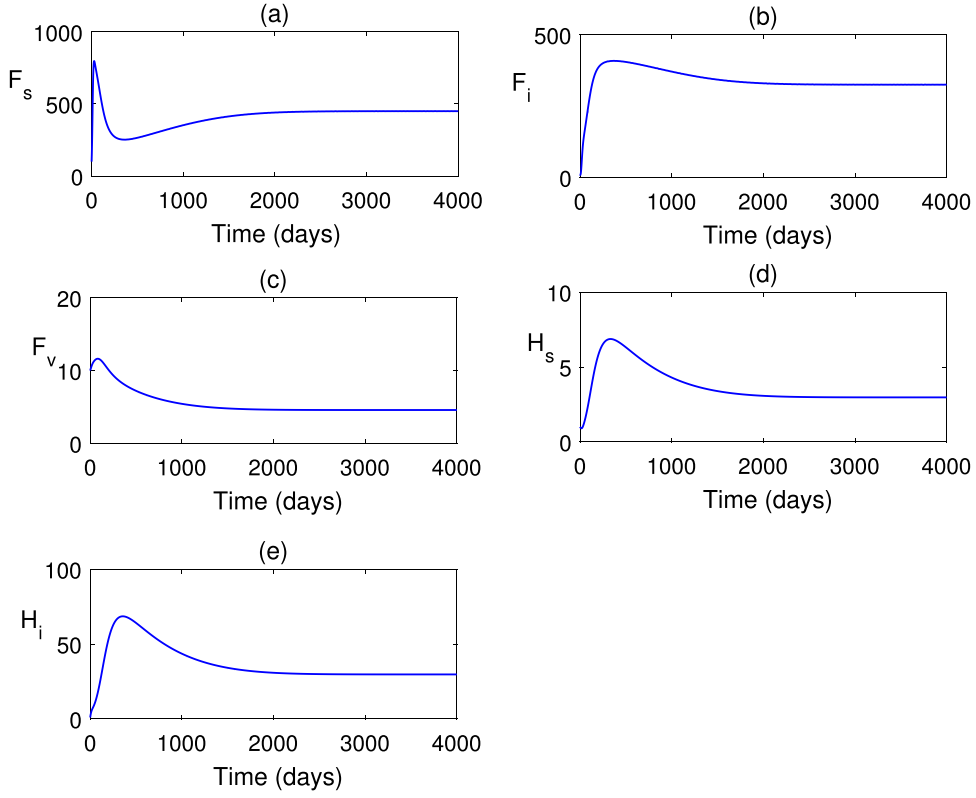

Fig. 5. Numerical solution of system (4.1) using the parameters given in Table 1.

$$\frac{dF_v}{dt} = \psi F_s - \theta_1 F_v(H_s + H_i) - \phi F_v, \tag{5.1c}$$

$$\frac{dH_s}{dt} = r_2(H_s + H_i)\left(1 - \frac{H_s + H_i}{k_2}\right) - \alpha\theta_1 F_i H_s + \omega H_i, \tag{5.1d}$$

$$\frac{dH_i}{dt} = \alpha\theta_1 F_i H_s - \delta H_i - \omega H_i, \tag{5.1e}$$

$$\frac{dM}{dt} = \beta H_i - \mu M. \tag{5.1f}$$

For the analysis of the system (5.1), we need the following invariant region:

$$\mathcal{B} = \Big\{(F_s, F_i, F_v, H_s, H_i, M) \in \mathcal{R} : 0 \le F_s + F_i + F_v \le k_1,$$

$$0 \le H_s + H_i \le k_2, H_i \le \frac{\alpha\theta k_1 k_2}{\delta+\omega},\ 0 \le M \le m\Big\}, \tag{5.2}$$

where

$$m = \frac{\beta\alpha\theta k_1 k_2}{(\delta+\omega)\mu}. \tag{5.3}$$

The Jacobian matrix for the model (5.1) is given by

$$J^{IV} = \begin{bmatrix} j_{11} & r_1\left(1-\frac{2(F_s+F_i)}{k_1}\right) & -\theta_1 F_s & -\theta_1 F_s & -\gamma F_s \\ \gamma M & -\theta_1 H_i - \theta_1 H_s - \epsilon & -F_i\theta_1 & -F_i\theta_1 & \gamma F_s \\ 0 & -\alpha\theta_1 H_s & j_{33} & r_2\left(1-\frac{2(H_s+H_i)}{k_2}\right) & 0 \\ 0 & \alpha\theta_1 H_s & \alpha\theta_1 F_i & -\delta & 0 \\ 0 & 0 & 0 & \beta & -\mu \end{bmatrix},$$

where

$$j_{11} = r_1\left(1-\frac{2(F_s+F_i)}{k_1}\right) - \theta_1 H_s - \theta_1 H_i - \gamma M,$$
$$j_{33} = r_2\left(1-\frac{2(H_s+H_i)}{k_2}\right) - \alpha\theta_1 F_i.$$

The Jacobian matrix at E_0^{IV} is given by

$$J_0^{IV} = \begin{bmatrix} r_1 & r_1 & 0 & 0 & 0 \\ 0 & -\epsilon & 0 & 0 & 0 \\ 0 & 0 & r_2 & r_2 & 0 \\ 0 & 0 & 0 & -\delta & 0 \\ 0 & 0 & 0 & \beta & -\mu \end{bmatrix}.$$

The eigenvalues of J_0 are $r_1, -\epsilon, r_2, -\delta, -\mu$, so E_0^{IV} is always unstable.

The Jacobian matrix at E_1^{IV} is given by

$$J_1^{IV} = \begin{bmatrix} -r_1 & -r_1 & -k_1\theta_1 & -k_1\theta_1 & -\gamma k_1 \\ 0 & -\epsilon & 0 & 0 & \gamma k_1 \\ 0 & 0 & r_2 & r_2 & 0 \\ 0 & 0 & 0 & -\delta & 0 \\ 0 & 0 & 0 & \beta & -\mu \end{bmatrix}.$$

The eigenvalues of J_1 are $-r_1, -\epsilon, r_2, -\delta, -\mu$, so E_1^{IV} is always unstable.

The Jacobian matrix at E_2^{IV} is given by

$$J_2^{IV} = \begin{bmatrix} -k_2\theta_1 + r_1 & r_1 & 0 & 0 & 0 \\ 0 & -k_2\theta_1 - \epsilon & 0 & 0 & 0 \\ 0 & -\alpha k_2\theta_1 & -r_2 & -r_2 & 0 \\ 0 & \alpha k_2\theta_1 & 0 & -\delta & 0 \\ 0 & 0 & 0 & \beta & -\mu \end{bmatrix}.$$

The eigenvalues of J_2^{IV} are $r_1 - k_2\theta_1, -k_2\theta_1 - \epsilon, -r_2, -\delta, -\mu$. Therefore, the system is stable if and only if $r_1 < k_2\theta_1$.

Fig. 6 illustrates the results from system (5.1). Small oscillations appear initially before the system approaches a coexistence steady state.

6. Model V: Molluscicide and logistic human growth with impulsive snail control

Snail control is conducted using molluscicide in fish ponds and canals [35]. Molluscicides are most commonly applied at discrete (rather than continuous) times, in order to avoid environmental toxicity. This can be modelled as an *impulsive effect* [36,37]. Suppose that the molluscicide is applied at t_k ($k \in \mathbb{N}$), and the elimination rate of snails at time t_k is q. With these assumptions, model (5.1) reduces to

$$\frac{dF_s}{dt} = r_1(F_s+F_i+F_v)\left(1-\frac{F_s+F_i+F_v}{k_1}\right) - \theta_1 F_s(H_s+H_i) - \gamma F_s M - \psi F_s, \tag{6.1a}$$
$$\frac{dF_i}{dt} = \gamma F_s M - \theta_1 F_i(H_s+H_i) - \epsilon F_i, \tag{6.1b}$$
$$\frac{dF_v}{dt} = \psi F_s - \theta_1 F_v(H_s+H_i) - \epsilon F_v, \tag{6.1c}$$
$$\frac{dH_s}{dt} = r_2(H_s+H_i)\left(1-\frac{H_s+H_i}{k_2}\right) - \alpha\theta_1 F_i H_s + \omega H_i, \tag{6.1d}$$
$$\frac{dH_i}{dt} = \alpha\theta_1 F_i H_s - \delta H_i - \omega H_i, \tag{6.1e}$$
$$\frac{dM}{dt} = \beta H_i - \mu M \qquad t \ne t_k, \tag{6.1f}$$
$$\Delta M = -qM \qquad t = t_k. \tag{6.1g}$$

Taking the maximal number of infected molluscs as an upper bound, the one-dimensional impulsive differential equation takes the form:

$$\frac{dM}{dt} = m - \mu M, \text{ for } t \ne t_k$$
$$\Delta M = -qM, \text{ for } t = t_k \text{ where } k = 1, 2, 3, \ldots \tag{6.2}$$

where m is defined in (5.3).

For a single impulsive cycle $t_k \le t \le t_{k+1}$, the endpoints of Eq. (6.2) satisfy

$$M(t_{k+1}^-) = \frac{m}{\mu}\left[1-e^{-\mu(t_{k+1}-t_k)}\right] + M(t_k^+)e^{-\mu(t_{k+1}-t_k)}.$$

Here, $M(t_k^-)$ and $M(t_k^+)$ represent number of infected molluscs immediately before and after the impulse therapy respectively.

Solving the recurrence relation, we have

$$\begin{aligned} M(t_n^-) = \frac{m}{\mu}\Big[&(1-q)^{(n-1)}e^{-\mu(t_n-t_1)} + (1-q)^{(n-2)}e^{-\mu(t_n-t_2)} \\ &+ \cdots + (1-q)e^{-\mu(t_n-t_{n-1})} \\ &+ 1 - (1-q)^{(n-2)}e^{-\mu(t_n-t_1)} - (1-q)^{(n-3)}e^{-\mu(t_n-t_2)} \\ &- \cdots - e^{-\mu(t_n-t_{n-1})}\Big] \end{aligned} \tag{6.3}$$

and

$$\begin{aligned} M(t_n^+) = \frac{m}{\mu}\Big[&(1-q)^n e^{-\mu(t_n-t_1)} + (1-q)^{(n-1)}e^{-\mu(t_n-t_2)} \\ &+ \cdots + (1-q)^2 e^{-\mu(t_n-t_{n-1})} \\ &- (1-q)^{(n-1)}e^{-\mu(t_n-t_1)} - (1-q)^{(n-2)}e^{-\mu(t_n-t_2)} \\ &- \cdots - (1-q)e^{-\mu(t_n-t_{n-1})} \\ &+ (1-q)\Big]. \end{aligned} \tag{6.4}$$

The solutions given in (6.3) and (6.4) can help to predict the infected molluscs present just before and after the nth impulse. However, these require the entire history of molluscicide application to be known, which is unlikely to be available.

If the time period $\tau = t_{n+1} - t_n$ is fixed, then we have

$$\begin{aligned} M(t_n^-) &= \frac{m}{\mu}\Big[1 + (1-q)e^{-\mu\tau} + (1-q)^2 e^{-2\mu\tau} + ... + (1-q)^{n-1}e^{-(n-1)\mu\tau} \\ &\quad - e^{-\mu\tau}\Big(1 + (1-q)e^{-\mu\tau} + ... + (1-q)^{n-2}e^{-(n-2)\mu\tau}\Big)\Big], \\ &= \frac{m}{\mu}\Big[\frac{1-(1-q)^n e^{-n\mu\tau}}{1-(1-q)e^{-\mu\tau}} - e^{-\mu\tau}\frac{1-(1-q)^{n-1}e^{-(n-1)\mu\tau}}{1-(1-q)e^{-\mu\tau}}\Big]. \end{aligned}$$

Therefore,

$$\begin{aligned} \lim_{n\to\infty} M(t_n^-) &= \frac{m}{\mu}\Big[\frac{1}{1-(1-q)e^{-\mu\tau}} - e^{-\mu\tau}\frac{1}{1-(1-q)e^{-\mu\tau}}\Big], \\ &= \frac{m}{\mu}\Big[\frac{1-e^{-\mu\tau}}{1-(1-q)e^{-\mu\tau}}\Big]. \end{aligned}$$

This is the maximum number of infected molluscs in the long term before applying the molluscicide.

After applying the molluscicide, the number of the infected molluscs is expressed by

$$\lim_{n\to\infty} M(t_n^+) = (1-q)\lim_{n\to\infty} M(t_n^-),$$

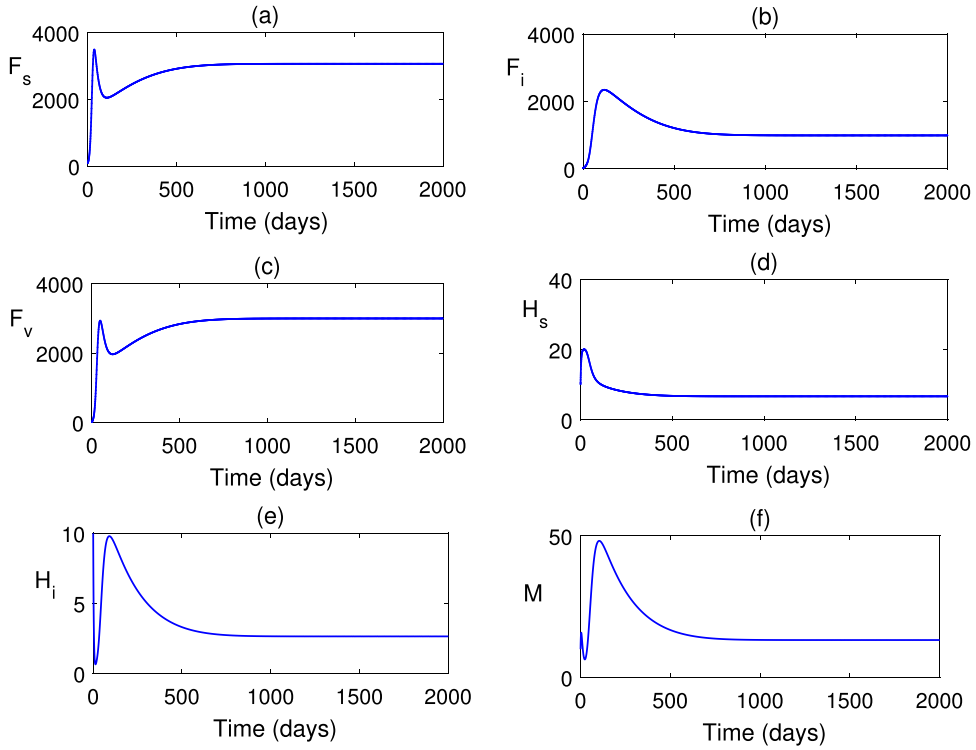

Fig. 6. Numerical solution of the system (5.1) using the parameters given in Table 1.

$$= (1-q)\frac{m}{\mu}\left[\frac{1-e^{-\mu\tau}}{1-(1-q)e^{-\mu\tau}}\right].$$

This is the long-term minimum number of infected molluscs.

Suppose $\tilde{M}$ is the maximum acceptable level of infected molluscs. After long-term molluscicide application, in order to keep the infected molluscs below $\tilde{M}$, we need the maximum time interval, τ_{max}, between two consecutive impulses to satisfy

$$(1-q)\frac{m}{\mu}\left[\frac{1-e^{-\mu\tau}}{1-(1-q)e^{-\mu\tau}}\right] < \tilde{M}.$$

Hence

$$\tau < \frac{1}{\mu}\ln\left[\frac{\tilde{M}\mu-(1-q)m}{(1-q)(m-\tilde{M}\mu)}\right] = \tau_{max}. \tag{6.5}$$

From (6.5), we have the maximum time interval of molluscicide application that will keep the infected molluscs below any arbitrary level $\tilde{M}$. However, we cannot clear the molluscs entirely without spraying infinitely often, which is not feasible (and the impulsive assumptions do not apply, in any case).

Fig. 7 illustrates system (6.1), showing the effect of applying impulsive control (in red). The impulsive molluscicides quickly control the infection if applied frequently enough.

7. Model behaviour comparison

Comparing the coexistence equilibria of model (2.1) with model (4.1), the susceptible human population is bounded. This is notable for model (2.1), where the human growth rate is assumed to be of Malthus type. However, the presence of the other populations keeps the possible explosion of the humans in check.

The disease is endemic in both situations, with all populations thriving. However, the presence of a carrying capacity k_2 for humans induces a slightly higher equilibrium level, mainly in the infected human subpopulation, and consequently also in their cumulative numbers. The human carrying capacity entails a higher prevalence for the logistic case; it is roughly $3/(3+4) = 0.43$, while for the Malthus case, it reduces to $1/(3+1) = 0.25$. The mollusc population settles at a higher level in the logistic case, from 10 to 30. The susceptible fish population is significantly reduced, from 700 in the Malthusian formulation to about 500 for the human logistic case. The prevalence in the two cases is respectively $200/(700+200) = 0.22$ and $350/(500+350) = 0.41$. Thus the introduction of the human logistic behaviour actually worsens the epidemic situation for the fish.

Comparing instead (3.1) to (2.1), the susceptible human population is also bounded, and the disease is endemic. However, the presence of the fish vaccination induces a higher equilibrium level for the humans, in both subpopulations of healthy and infected, and consequently also in their cumulative numbers. However, with the human carrying capacity, the disease attains a higher prevalence; it is roughly $3/(3+7) = 0.3$ in the latter case and $1/(3+1) = 0.25$ in the former. The mollusc population is higher in the vaccination case, raising to a value around 17 from 10. The fish population benefits the most from the introduction of the vaccination policy, which is not unexpected. It jumps from about 900 to 7000, with the prevalence exhibiting a moderate decrease, from $200/900 = 0.22$ to $1000/7000 = 0.14$.

We now compare models (4.1) and (5.1). Both contain the human population dynamics formulated via a logistic model, but a molluscicide is used in the second one. Molluscs are reduced from 30 to a value around 15. For the human population, the changes are very small for both susceptible and infected individuals, entailing also little change in the disease prevalence. For the healthy fish, there is a sixfold raise if vaccination is applied, from 500 to 3000. Their overall population also experiences a large increase, from 900 to 7000. The fish disease prevalence drops dramatically from $400/900 = 0.44$ to $1000/7000 = 0.14$.

We now consider models (3.1) and (5.1) where vaccination is used in both, but the former has a Malthusian formulation for the humans, and the latter has a logistic formulation. The mollusc population does not show any significant change. The humans are at level 10 in the former case, and about the same in the latter. This is true for both healthy and infected subpopulations, which implies that the disease prevalence does not change, remaining at level $3/(3+7) = 0.3$. Infected

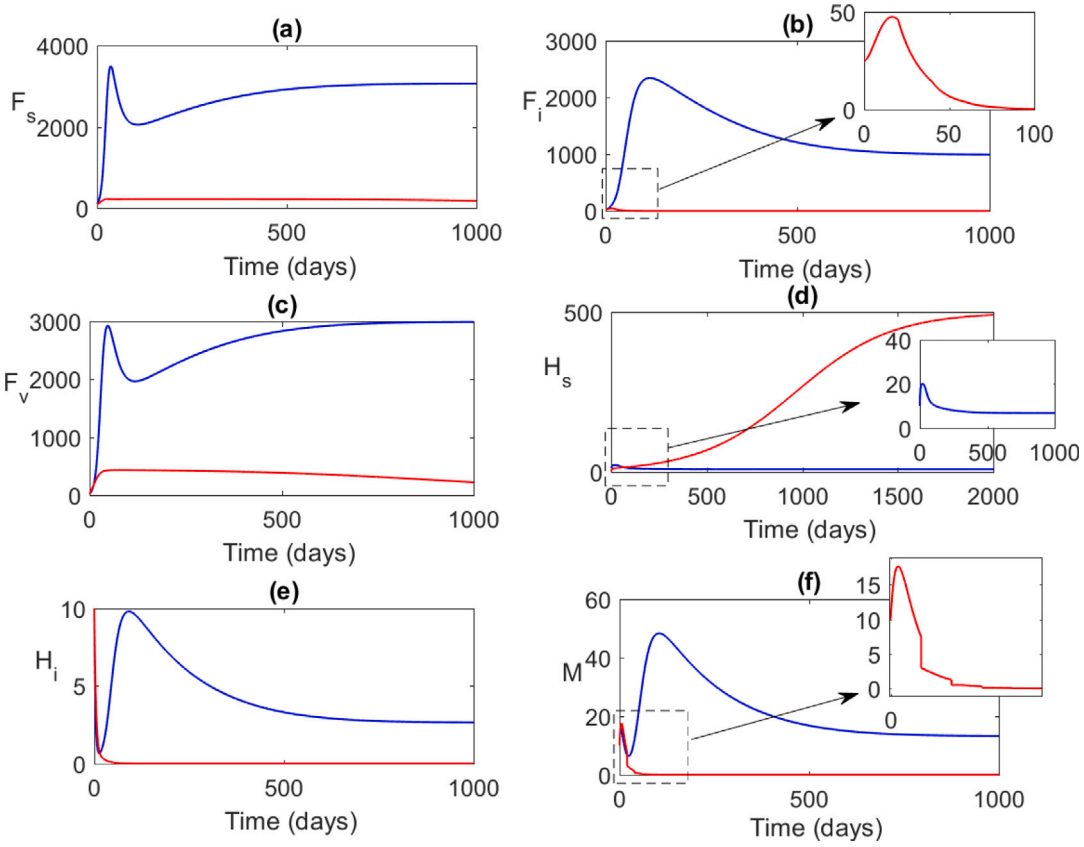

Fig. 7. Numerical solution of the system (6.1) using the parameters given in Table 1 and $q = 0.2$, $\tau = 2$. Blue curves denote the system without impulses and red curves denote the system with impulsive control. (For interpretation of the references to colour in this figure legend, the reader is referred to the web version of this article.)

fish are 1000 in the former case, with a prevalence of $1000/7000 = 0.14$, and the situation does not seem to change much in the second case.

Finally, we take into consideration the model with impulsive snail control, system (6.1). This policy allows us to keep all infected populations in check. Essentially, the molluscs are controlled (albeit not eradicated), and the infection is eliminated in humans. The enlargements of Fig. 7 show that there is indeed a small epidemic outbreak in both humans and fish before the disease gets eradicated. However, in comparison with the model without impulses (5.1), the peaks are reduced by a factor of 40 for the fish and somewhat reduced for the other two populations. In all the populations, the disease is extinguished quickly, in a smooth decreasing fashion.

8. Discussion

Clonorchiasis has been recognized as a neglected tropical disease by the World Health Organization for decades and remains prevalent worldwide. Clinical and epidemiological research into clonorchiasis over the past 140 years has contributed to a deeper understanding of the parasite, intermediate hosts and disease [38,39]. Most of the clonorchiasis studies focus on the discovery of new diagnostic, drug and vaccine targets, as well as the pathology and the biology of the disease. Relatively few studies have used mathematical models to assess strategies for large-scale control of clonorchiasis.

We studied the dynamics of clonorchiasis using four deterministic mathematical models to describe the human-snail-fish transmission of clonorchiasis. Our models examined the current control and prevention policies and incorporated impulsive snail control strategy for reducing the transmission of clonorchiasis. We also derived the reproduction number for the general epidemic model. Using the theory of impulsive differential equations, we found an extinction threshold for the disease, along with the maximum interval of applying molluscicides. We also performed numerical simulations to examine multiple scenarios and found that fish vaccination and snail control are both viable strategies.

Other possible intervention methods could include sanitary deconfinement [40] or mimicking the control used for COVID-19 [41]. A potential modelling direction is to develop a digital twin for clonorchiasis, linking timescales of system time and slow time [42].

Due to the neglect and absence of systematic interventions, clonorchiasis remains prevalent worldwide, although some chemotherapy and control programmes have been implemented over several years in a few endemic areas [18,43]. Further research is needed to increase the number of models and to address the neglect of this disease in the field.

CRediT authorship contribution statement

Mainul Haque: Co-designed the study. **Fahad Al Basir:** Mathematical analysis, Numerical simulations. **Ezio Venturino:** Edited the manuscript. **Abdulhalim Saeed:** Mathematical analysis, Numerical simulations. **Stacey R. Smith?:** Co-designed the study, Wrote the introduction, Edited the manuscript.

Declaration of competing interest

The authors declare that they have no known competing financial interests or personal relationships that could have appeared to influence the work reported in this paper.

Data availability

No data was used for the research described in the article.

Acknowledgements

The authors are grateful to Weihua Meng and Gabriel DeRooy for technical assistance. SRS? is supported by an NSERC Discovery Grant. For citation purposes, please note that the question mark in "Smith?" is part of her name.

References

[1] Kim T-S, Pak JH, Kim J-B, Bahk YY. Clonorchis sinensis, an oriental liver fluke, as a human biological agent of cholangiocarcinoma: a brief review. BMB Rep 2016;49(11):590–7.
[2] Lun Z-R, Gasser RB, Lai D-H, Li A-X, Zhu X-Q, Yu X-B, Fang Y-Y. Clonorchiasis: a key foodborne zoonosis in China. Lancet Infect Dis 2005;5:31–41.
[3] Keiser J, Utzinger J. Food-borne trematodiasis: current chemo- therapy and advances with artemisinins and synthetic trioxolanes. Trends Parasitol 2007;23(11):555–62.
[4] Qian MB, Utzinger J, Keiser J, Zhou XN. Clonorchiasis. Lancet 2016;387(10020):800–10.
[5] Liang C, Hu XC, Lv ZY, Wu ZD, Yu XB, Xu J, Zheng HQ. Experimental establishment of life cycle of Clonorchis sinensis. Chin J Parasitol Parasit Dis 2009;27(2):148–50.
[6] Li S, Chung Y-B, Chung B-S, Choi M-H, Yu J-R, Hong S-T. The involvement of the cysteine proteases of Clonorchis sinensis metacercariae in excystment. Parasitol Res 2004;93(1):36–40.
[7] Attwood HD, Chou ST. The longevity of Clonorchis sinensis. Pathology 1978;10(2):153–6.
[8] Kim J-H, Choi M-H, Bae YM, Oh J-K, Lim MK, Hong S-T. Correlation between discharged worms and fecal egg counts in human clonorchiasis. PLoS Negl Trop Dis 2011;5(10):e1339.
[9] Lin R-Q, Tang J-D, Zhou D-H, Song H-Q, et al. Prevalence of Clonorchis sinensis infection in dogs and cats in subtropical southern China. Parasites Vectors 2011;4:180.
[10] Control of foodborne trematode infections. World Health Organization; 1995.
[11] Keiser J, Xiao S-H, Smith TA, Utzinger J. Combination chemotherapy against Clonorchis sinensis: Experiments with artemether, artesunate, OZ78, praziquantel, and tribendimidine in a rat model. Antimicrob Agents Chemother 2009;53(9):3770–6.
[12] Chai J-Y. Praziquantel treatment in trematode and cestode infections: An update. Infect Chemother 2013;45(1):32–43.
[13] Chen M, Lu Y, Hua X, Mott KE. Progress in assessment of morbidity due to Clonorchis sinensis infection: A review of recent literature. World Health Organization; 1994.
[14] Keiser J, Utzinger J. Chemotherapy for major food-borne trematodes: a review. Expert Opin Pharmacother 2004;5(8):1711–26.
[15] Nissen S, Nguyen LAT, Thamsborg SM, Dalsgaard A, Johansen MV. Reinfection of dogs with fish-Borne zoonotic trematodes in Northern Vietnam following a single treatment with praziquantel. Plos Negl Trop Dis 2014;8(1):e2625.
[16] Tang Z, Huang Y, Yu X-B. Current status and perspectives of clonorchis sinensis and clonorchiasis: epidemiology, pathogenesis, omics, prevention and control. Infect Dis Poverty 2016;5:71.
[17] Yuan R, Huang J, Zhang X, Ruan S. Modeling the transmission dynamics of Clonorchiasis in Foshan, China. Sci Rep 2018;8:15176.
[18] Sithithaworn P, Andrews RH, Nguyen VD, Wongsaroj T, Sinuon M, Odermatt P, et al. The current status of opisthorchiasis and clonorchiasis in the Mekong Basin, Paiboon. Parasitol Int 2012;61(1):10–6, Sithithaworn and Ross H. Andrews and Nguyen Van De et al.
[19] He YT, Huang XH, Fang YY, Zeng QS, Li LD, Luo L, Lai YS. Cost-effectiveness evaluation of different control strategies for Clonorchis sinensis infection in a high endemic area of China: A modelling study. PLOS Negl Trop Dis 2022;16(5):e0010429.
[20] Song K-W, Kang S-Y, Lee S-H. A mathematical approach to the mode of transmission of Clonorchiasis in the inhabitants of Nak-dong and Han River Basin. Korean J Parasitol 1979;17(2):114–20.
[21] Keiser J, Utzinger J. Emerging foodborne trematodiasis. Emerg Infect Diseases 2005;11(10):1507–14.
[22] Qian M-B, Chen Y-D, Fang Y-Y, et al. Disability weight of clonorchis sinensis infection: Captured from community study and model simulation. PLoS Negl Trop Dis 2011;5(12):e1377.
[23] Lai Y. Bayesian geostatistical and mathematical models to assess the geographical distribution of neglected tropical diseases. Universität Basel; 2016.
[24] Gao S, Yuan R, Liu Y, Meng X. Modelling the effects of snail control and health education in Clonorchiasis infection in Foshan, China. Complexity 2019;2019.
[25] Zhang T, Li Z, Ma L, Song X. Threshold dynamics in a clonorchiasis model with time delays. Appl Math Model 2022;102:351–70.
[26] Vonghachack Y, Odermatt P, Taisayyavong K, Phounsavath S, Akkhavong K, Sayasone S. Transmission of Opisthorchis viverrini, Schistosoma mekongi and soil-transmitted helminthes on the Mekong Islands, Southern Lao PDR. Infect Dis Poverty 2017;6(1):1–5.
[27] Smout MJ, Laha T, Mulvenna J, Sripa B, Suttiprapa S, Jones A, Brindley PJ, Loukas A. A granulin-like growth factor secreted by the carcinogenic liver fluke, Opisthorchis viverrini, promotes proliferation of host cells. PLoS Pathog 2009;5(10):e1000611.
[28] Brockelman WY, Upatham ES, Viyanant V, Ardsungnoen S, Chantanawat R. Field studies on the transmission of the human liver fluke, opisthorchis viverrini, in northeast thailand: population changes of the snail intermediate host. Int J Parasitol 1986;16(5):545–52.
[29] Bürli C, Harbrecht H, Odermatt P, Sayasone S, Chitnis N. Mathematical analysis of the transmission dynamics of the liver fluke, Opisthorchis viverrini. J Theoret Biol 2018;439:181–94.
[30] Phongluxa K, van Eeuwijk P, Soukhathammavong PA, Akkhavong K, Odermatt P. Perceived illness drives participation in mass deworming cam-paigns in laos. Acta Trop 2015;141(Part B):281–8.
[31] Anderson RM, May RM. Helminth infections of humans: mathematical models, population dynamics, and control. Adv Parasitol 1985;24. 1-01.
[32] Anderson RM, May RM. Infectious diseases of humans: Dynamics and control. Oxford University Press; 1992.
[33] Chen Z, Zou L, Shen D, Zhang W, Ruan S. Mathematical modelling and control of Schistosomiasis in Hubei Province, China. Acta Trop 2010;115(1–2):119–25.
[34] Spear RC, Hubbard A, Liang S, Seto E. Disease transmission models for public health decision making: toward an approach for designing intervention strategies for Schistosomiasis japonica. Environ Health Perspect 2002;110(9):907.
[35] McCullough FS, Gayral PH, Duncan J, Christie JD. Molluscicides in schistosomiasis control. Bull World Health Organ 1980;58(5):681, World Health Organization.
[36] Bainov D, Simeonov PS. Systems with impulse effect: Stability, theory, and applications. Ellis Horwood; 1989.
[37] Bainov D, Simeonov PS. Impulsive differential equations: Asymptotic properties of the solutions, Vol. 28. World Scientific; 1995.
[38] Bouvard V, Baan R, Straif K, Grosse Y, et al. A review of human carcinogens-Part B: biological agents. Lancet Oncol 2009;10:321–2.
[39] Fürst T, Keiser J, Utzinger J. Global burden of human food-borne trematodiasis: a systematic review and meta-analysis. Lancet Infect Dis 2012;12:210–21.
[40] Silva CJ, Cruz C, Torres DF, Munuzuri AP, et al. Optimal control of the COVID-19 pandemic: controlled sanitary deconfinement in Portugal. Sci Rep 2021;11(1):1–5.
[41] Saha S, Smanta G, Nieto JJ. Impact of optimal vaccination and social distancing on COVID-19 pandemic. Math Comput Simulation 2022;200:285–314.
[42] Area I, Fernández FJ, Nieto JJ, Tojo FA. Concept and solution of digital twin based on a stieltjes differential equation. Math Methods Appl Sci 2022.
[43] Qian M, Chen Y, Song L, Yang G, Zhou X. The global epidemiology of clonorchiasis and its relation with cholangiocarcinoma. Infect Dis Poverty 2012;1:4.